IDENTIFICATION OF CHARACTERISTIC PARAMETERS FOR HYDROSTATIC BEARINGS

Y. Kang * **S.-Y. Hu** **Y.-P. Chang** **T.-P. Wang**

Department of Mechanical Engineering
Chung Yuan Christian University
Chung-Li, Taiwan

ABSTRACT

This study proposes a method to identify the characteristic parameters of hydrostatic bearing. When load or supply pressure changed, the inlet and outlet pressures of restrictor, flow rate and worktable displacement are examined for establish identification equations. The practical values of the characteristic parameters can be obtained by minimizing the differences between measure flow rate and identify flow rate. The differences between practical and design values of these parameters can be used to calibrate design parameters for satisfying the requirements.

Keywords: Hydrostatic bearing, Identification, Characteristic parameters.

1. INTRODUCTION

Raimondi and Boyd [1], Malanoski and Loeb [2], and Rippel [3,4] investigated the static characteristics and optimization of design parameters on hydrostatic bearing using three types of constant restrictors. Kang *et al*. [5-8] investigated the static characteristics of open-type and closed-type planar bearings compensated by the constant compensations and variable restrictors to give that the bearing characteristics is determined by bearing design and the match of bearing and compensation. They revealed that variable compensations achieved infinite and negative stiffnesses at certain pressure ratio when specific compliances of active element are used.

O'Donoghue and Rowe [9], Rowe and O'Donoghue [10], Yakir [11] presented design the strategy and procedures for hydrostatic slideway to use for machine tool. Telingater [12] investigated the three shapes of recesses in the hydrostatic slideways by the analytical and experimental methods. Bushuyev [13] investigated the influences of the recess numbers on tilt of planar slideway by analysis. Sharma *et al*. [14] utilized finite element method to analyze the thrust bearings of four shapes in comparisons of the static characteristics. Kang *et al*. [15] investigated the influences of constant compensations on the dynamic characteristics of a circular worktable supported by a closed-type hydrostatic thrust bearing.

However, between determined values and practical values of the characteristics have large differences because manufacturing errors and disregard in design formula. Kang *et al*. studied the finite element models [16] of the membrane-type restrictor and [17] a network model of flow resistances, the modification of both models due to experimental data have been presented. Kang *et al*. [18] presented an approach to identify the restriction parameter and membrane deformation coefficient of single-action membrane-type restrictor by experimental results which are measurements of the inlet pressure, the outlet pressure and the flow rate of restrictor.

This paper studies the method to identify characteristic parameters which are restriction constant of the bearing pad, restriction constant of connecting pipe, initial film thickness with respect to the supply pressure, effective area of the bearing pad, and the variations of recess pressures by the loads change. The identification equations are derived from flow continuity equations, which are obtained by minimizing the error squares between identified and measured flow rates. The coupled equations for identifying recess pressure and restriction constant of connecting pipe can be solved by utilizing the measurements of flow rate, inlet and outlet pressures of each restrictor. The coupled equations for identifying initial film thickness and restriction constant of bearing pad can be solved by utilizing the measurements of worktable displacements, recess pressures and flow rates of each restrictor. The coupled equations for identifying effective areas of each pad can be solved by utilizing recess pressures to minimize the error squares between identified and measured the loads.

The three practical bearings using the same hydrostatic system are investigated in case studies. Two bearings have different the circular pads and recesses designs and another is rectangular bearing. In these cases, the comparison between both results of identification and determination reveals that characteristic parameters of hydrostatic bearing can be obtained by identification method of this study. Since identification results give the differences between designs and

* Corresponding author (yk@cycu.edu.tw)

DOI : 10.1017/jmech.2014.91
Copyright © 2015 The Society of Theoretical and Applied Mechanics, R.O.C.
https://doi.org/10.1017/jmech.2014.91 Published online by Cambridge University Press

practical values of characteristic parameters to offer a powerful calibration facility allowing designers to find exact matches for the requirement of bearing characteristics. Further, identification results due to the various designs can give the influence of design parameters, such as oil return grooves and bearings without groove, recess numbers and shapes, sill sizes and shapes, the bearing characteristics of all types.

2. PRINCIPLES

The pressurized fluid of hydrostatic bearing is externally supplied by the hydraulic pump and is passed through the restrictors to be compensated by the recess pressures. The recess pressures can change by the loads applied on the worktable and fed into bearing recesses. When the fluid is flowing out sill from recess, it forms a film to separate both solid surfaces of the worktable and bearing pad. The pad is a composite of the recess and sill (or named by land), which can manufacture on the worktable or on the bearing. The illustration of an open-type hydrostatic system can be seen in Fig. 1, the working fluid is pressurized to P_s and compensated to P_r of pressure and T_r of temperature by restrictor. The reduction from P_r to P_r' of the pressure is caused by flow resistances of connecting pipes. The flow is fed into recess to the recess pressure P_r' to construct a hydrostatic oil film between the bearing sill and the lower surface of worktable. This film is utilized to support the gross load that includes of the worktable weight W_0 and applied load W. T_r' and T_0 are average temperatures that can be measured before the inlet and outlet of the bearing, respectively.

2.1 Identification of the Restriction Constant of Connecting Pipe and the Recess Pressure

The flow rate passing through the connecting pipe is proportional to the difference between inlet and outlet pressures of the connecting pipe, which can be determined by

$$Q = \kappa_\mu (P_r - P_r') = \frac{\kappa}{\mu}(P_r - P_r') \tag{1}$$

where $\kappa_\mu = \dfrac{\pi D_p^4}{128 \mu L_p}$ (unit: $m^5/N{\cdot}s$) is restriction parameter, $\kappa = \mu\kappa_\mu$ is restriction constant of the connecting pipe, μ is dynamic coefficient of viscosity that can be determined by ASTM D341 formulas , which are using the average temperature between the inlet and outlet of connecting pipe (T_r and T_r').

Usually recess pressure P_r' can be measured directly, but additional holes for measuring pressures maybe induce weakness and leakage. So we presented the recess pressures can be obtained by the identification Eq. (1) which is using the measurements of P_r and flow rate Q. Also, restriction constant of connecting pipe κ can be obtained at the same time.

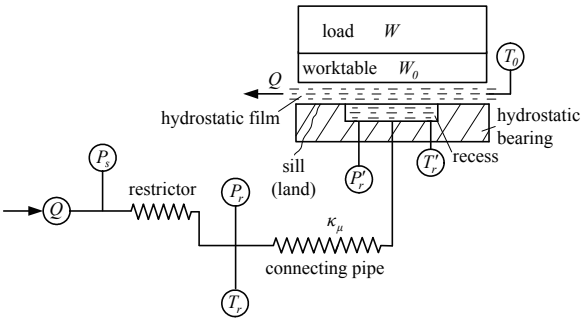


Fig. 1 An open-type hydrostatic bearing.

Changing supply pressure and the constant load can get constant recess pressure, but can induce the variation of outlet pressure of restrictor. Each load measures the N times outlet pressures and flow rates along with the N times changes of supply pressures. Q_j is expressed to the j-th measured flow rate and Q_j' is obtained from identification corresponding to the j-th measured P_{rj} of recess pressure. The error between both flow rates is $e_j = Q_j' - Q_j$ and the error sum of square is

$$E = \sum_{j=1}^{N} e_j^2 = \sum_{j=1}^{N} (Q_j' - Q_j)^2 = \sum_{j=1}^{N} \left[\frac{\kappa}{\mu_j}(P_{rj} - P_r') - Q_j \right]^2 \tag{2}$$

Minimizing E with respect to both P_r' and κ uses regression analysis by N data of measurements to establish an identified equation, which gives

$$\frac{\partial E}{\partial \kappa} = 2\sum_{j=1}^{N} \left\{ \left[\frac{\kappa}{\mu_j}(P_{rj} - P_r') - Q_j \right] \times \frac{P_{rj} - P_r'}{\mu_j} \right\} = 0 \tag{3a}$$

$$\frac{\partial E}{\partial P_r'} = 2\sum_{j=1}^{N} \left\{ \left[\frac{\kappa}{\mu_j}(P_{rj} - P_r') - Q_j \right] \times \left(\frac{\kappa}{\mu_j} \right) \right\} = 0 \tag{3b}$$

where both Q_j and P_{rj} are measured by all of supply pressures and substituted into Eqs. (3a) and (3b), μ_j is determined by average temperature of j-th measurements of T_r' and T_r. Then, recess pressure P_r' and restriction constant of connecting pipe κ are obtained by solving simultaneously both Eqs. (3a) and (3b). κ is relation with connecting pipe diameter and length, and P_r' is work pressure which is must greater than zero. So solving κ and P_r' have physically meaningful solution that we needed is unique and the other solutions are the complex variables or negative.

2.2 Identification of Restriction Constant of Pad and Initial Film Thickness

The worktable has own weight W_0 which can compress the film to make an initial displacement d_0. So $h_0 - d_0$ is defined as the initial film thickness which is only subjected worktable weight. When a load is supported on this worktable, an additional displacement

https://doi.org/10.1017/jmech.2014.91 Published online by Cambridge University Press

d is induced as shown in Figure 2. For applying the sum of W_0 and the j-th applied load W_j on the worktable, d_j and h_j are respectively worktable displacement (measured) and film thickness (identified) due to W_j. For the recess pressure P_r', the flow rate can be

$$Q = \frac{P_r' h^3}{12\mu}\gamma = \frac{\gamma}{12\mu} P_r' [h_0 - d_0 - d]^3 \tag{4a}$$

qr

$$h_0 - d_0 = \sqrt[3]{\frac{12\mu Q}{P_r'\gamma}} + d \tag{4b}$$

where $h = (h_0 - d_0 - d)$ is film thickness, γ is restriction constant of a hydrostatic pad, and μ is determined by the average temperature of T_r' and T_0 of the r-th pad.

Regardless of the closed-type or open-type bearing, the practical and determined values of the restriction parameter γ doesn't be on all fours. Also, the practical value of initial film thickness $h_0 - d_0$ cannot be obtained from measuring or determining. Hence real γ and $h_0 - d_0$ should be identified in the experiments by the measurement of pressures, flow rates, and displacements. Experiments are by using the constant supply pressure P_s and varying the load W to change the film thickness h and recess pressure P_r'. As shown in Fig. 2, displacement meter is utilized to measure the change of the film thickness d_j with respect to the j-th load W_j. At the same time, flow rate Q_j and outlet pressure P_{rj} of restrictor are measured. By rearranging Eq. (1), the recess pressure P_r' expresses as $P_{rj}' = P_{rj} - \mu_j Q_j \kappa^{-1}$ with respect to the j-th load W_j.

For N' times changing P_s the sum of error squares between determined and measured values of the flow rate is

$$E = \sum_{j=1}^{N'} \left[\frac{\gamma}{12\mu_j} P_{rj}' (h_0 - d_0 - d_j)^3 - Q_j \right]^2 \tag{5}$$

where μ_j is the absolute viscosity corresponding to the average temperature of T_r' and T_0 in the j-th measurement. Minimizing the sum of error squares to give the coupled equations for identifying γ and $h_0 - d_0$ as

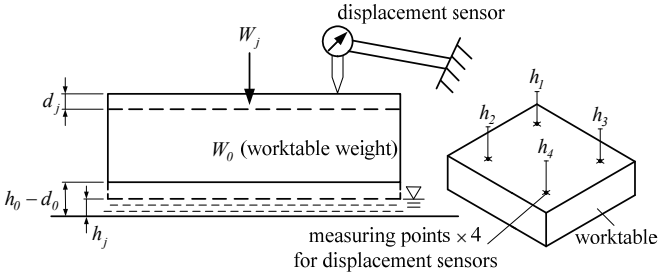


Fig. 2 Displacement measurement of worktable applied by load.

$$\frac{\partial E}{\partial (h_0 - d_0)} = 2\sum_{j=1}^{N'} \left\{ \left[\frac{\gamma}{12\mu_j} P_{rj}' (h_0 - d_0 - d_j)^3 - Q_j \right] \times \frac{\gamma P_{rj}'}{12\mu_j} \times 3(h_0 - d_0 - d_j)^2 \right\} = 0 \tag{6a}$$

$$\frac{\partial E}{\partial \gamma} = 2\sum_{j=1}^{N'} \left\{ \left[\frac{P_{rj}'\gamma}{12\mu_j} (h_0 - d_0 - d_j)^3 - Q_j \right] \frac{P_{rj}'}{12\mu_j} (h_0 - d_0 - d_j)^3 \right\} = 0 \tag{6b}$$

where $d_j = h_0 - d_0 - h_j$ is caused by adding load W_j. Substituting N times experimental data (Q_j、d_j、μ_j) and P_{rj}' to above equations and to solve simultaneously. γ is relation with bearing pad sizes, and $h_0 - d_0$ is film thickness which is must greater than zero. So solving γ and $h_0 - d_0$ have physically meaningful solution that we needed is unique and the other solutions are the complex variables or negative.

The worktable kept level in the start. The supply pressure can affect the recess pressure of the four pads and flow rates which made worktable can't keep level. The initial film thickness $h_0 - d_0$ of the four positions can't affect by film thickness therefore can't subject to the worktable tilting affect. Theoretically, the restriction constant of hydrostatic pad is a function of the length of sill and the recess area. When starting to add load, the tilting doesn't affect the formula of identification $h_0 - d_0$ and restriction constant γ of pad.

2.3 Identification of Effective Area and Load Sharing Ratio of Each Pad

The gross load applied on bearing can be expressed by

$$P_1' A_1 + P_2' A_2 + \cdots + P_n' A_n = W + W_0 \tag{7a}$$

where A_r is effective area and P_r' is recess pressure of the *r-th* pad and n is total number of pads. For the N times measuring P_{rj}' with respect to N times loading with various load W_j, the effective areas of the n pieces of pads can be identified and the applied load W_j can be determined by

$$W_j' = P_{1j}' A_1 + P_{2j}' A_2 + \cdots + P_{nj}' A_n - W_0 \tag{7b}$$

Thus, for N times load applying the total error square between estimated and practical loads is

$$E = \sum_{j=1}^{N} e_j^2 = \sum_{j=1}^{N} (P_{1j}' A_1 + P_{2j}' A_2 + \cdots + P_{nj}' A_n - W_0 - W_j)^2 \tag{8}$$

Minimizing E by the partial differentiating E with respect to the each A_r equates zero to give

$$\frac{\partial E}{\partial A_i} = 2\sum_{j=1}^{N} (P_{1j}' A_1 + P_{2j}' A_2 + \cdots + P_{nj}' A_n - W_0 - W_j) P_{ij}' = 0 \tag{9a}$$

https://doi.org/10.1017/jmech.2014.91 Published online by Cambridge University Press

or

$$A_1\sum_{j=1}^{N}P'_{1j}P'_{ij}+A_2\sum_{j=1}^{N}P'_{2j}P'_{ij}+\cdots+A_i\sum_{j=1}^{N}P'^{2}_{ij}$$
$$+\cdots+A_n\sum_{j=1}^{N}P'_{ij}P'_{nj}=\sum_{j=1}^{N}P'_{ij}(W_j+W_0) \qquad (9b)$$

Thus, all effective areas A_1, …, A_n can be obtained simultaneously by solving Eq. (9b). Furthermore, the average ratio of load sharing ratios of the i-th pad can be determined by

$$\alpha_i=\sum_{j=1}^{N}\left(\frac{P'_{ij}A_i}{W_j+W_0}\right)=\frac{A_i\sum_{j=1}^{N}P'_{ij}}{NW_0+\sum_{j=1}^{N}W_j} \qquad (10)$$

3. EXPERIMENTS ON IDENTIFICATION OF BEARING

An experimental installation for the bearing identification is illustrated in Fig. 3, which has supply pressurize oil circuit and hydrostatic system in the same. And the worktable on top with four pads to support vertical load and with two pads in zygomorphic both sides to keep worktable in the neutral position without contacting lateral sides. The connecting pipes numbered of 1 to 4 for connecting the side recesses and numbered of 5 to 8 for connecting the bottom pads which are identified. The pressurized oil is circulated from pump to pass through restrictors and connecting pipes, which reaches each recess and then flows out from the clearance between both surfaces of worktable and base.

This study utilizes a kind of the slideway oils which the viscosity is 68mm^2/s at 40°C. The oil passes through heat exchanger for keeping due to cooling before returning the oil reservoir and being pumped again that the temperature fluctuations of the oil at all measurement points can kept less than 2°C. For convenience in experimental setup, vertical load is applied on the top of worktable which induces changes of pressures and flow rates. The parameters of bottom vertical pads with their connecting pipes will be identified.

For identifying the pads, the pressures are measured at restrictor exit, flow rates are measured for each connecting pipe, and temperatures are measured at restrictor exits and recesses. Additionally, the four displacement meters are used to measure the vertical displacements of four corners on the worktable top. Pressure sensors locating on upstream of restrictors are used to regulate the supply pressure for each recess.

4. CASE STUDY

4.1 Hydrostatic Pads and Connecting Pipes

In this study, three designs of hydrostatic pads are used rectangular pads are fixed and unchangeable as shown in Fig. 4(a), and circular pads are attachable and

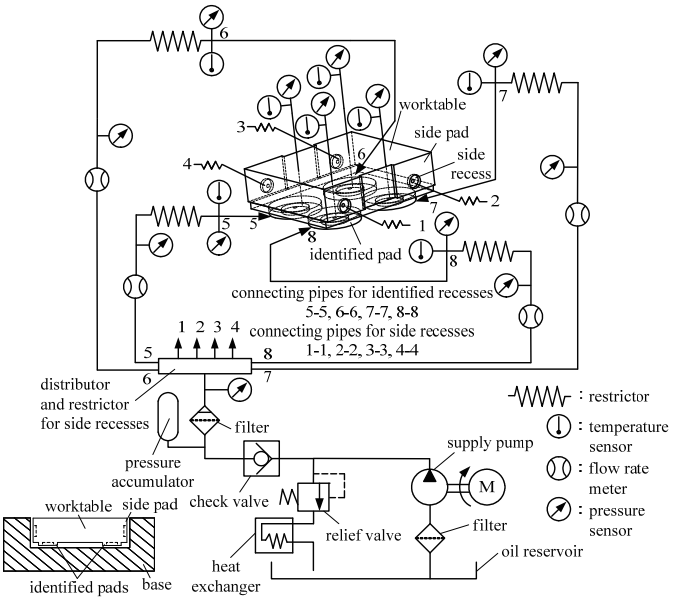


Fig. 3 Illustration of an experimental installation.

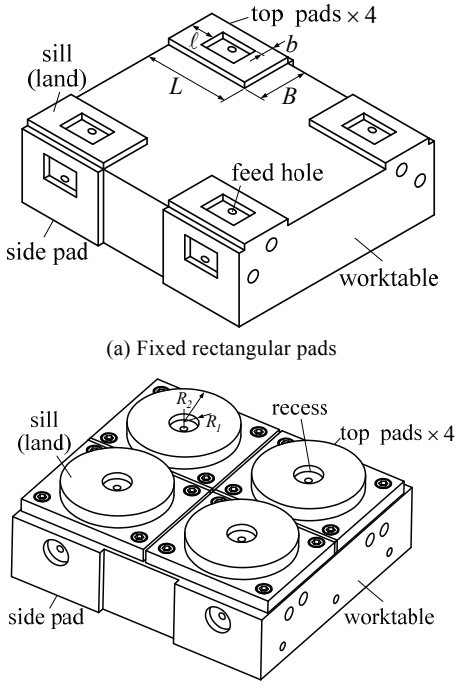


Fig. 4 Bearing configuration in an worktable with hydrostatic pads.

changeable as shown in Fig. 4(b). Their geometric parameters are described in Table 1 and for circular pads, outer diameter of pad is ϕ76mm and inner diameter has ϕ20 and ϕ60mm of two sizes recesses. Each pad is fixed on worktable by the four set screws which can be assembled to change pads. The gross weights of the worktable with four pads have three types to list in the fifth row of Table 1.

The restriction constants based on the flow theory can be determined individually by

$$\gamma=2\left(\frac{B-2b}{\ell}+\frac{L-2\ell}{b}\right) \qquad (11a)$$

https://doi.org/10.1017/jmech.2014.91 Published online by Cambridge University Press

Table 1 Design parameters and characteristic parameters of hydrostatic pads.

Design parameter \ Pad type	Rectangular pad (mm)	Circular pad (mm)	Circular pad (mm)
Recess size	20 × 30	ϕ20	ϕ60
Recess area (mm^2)	600	314	2826
Outer size of sill	40 × 70	ϕ76	ϕ76
Diameter of feed hole	ϕ5	ϕ5	ϕ5
Gross weight (N)	219	248	240
Restriction constant of pad	8	4.71	26.58
Effective area of pads (cm^2)	15	15.81	36.14

for rectangular pad, where B, L are recess width and length, b, ℓ are sill length, and

$$\gamma = \frac{2\pi}{\ell n \frac{R_2}{R_1}} \tag{11b}$$

for circular pad, where R_1 and R_2 both are radius of recess and pad respectively. The restriction constant for three types of pads are determined by using Eqs. (11a) and (11b) as shown in the sixth row of Table 1.

The connecting pipes utilized in this experimental installation have the same as diameter of $D_p = 6.35$mm, but have different lengths described in the second row of Table 2, and their restriction constants are determined by $\kappa = \pi D_p^4 / 128 L_p$ and listed on the third row of Table 2.

4.2 Identification Results

In experiments, the same 200N of weight is in sequence to add on the worktable. Where supply pressures P_{si}, restrictor outlet pressures P_{rj} and temperatures T_{rj}, flow rates Q_j, temperatures T_r' of pipe ends, and film temperature T_0 in outer periphery of bearing clearance are measured and recorded for all load adding. Also, each displacement due to add weight on worktable is measured in the corners of four positions as shown in Fig. 2 and their average is recorded. This process is repeated till total weight reaches already-decided value. Four supply pressures of P_s = 0.5, 1, 1.5, 2MPa are utilized at one load to give four sets of measurement data with respect to each P_s. The restrictor outlet pressures and flow rates can be risen by supply pressure increasing. However, the recess pressures are dependent only on applying load and cannot be changed by supply pressure.

Recess pressure P_r' and restriction constant κ of connecting pipes are determined by Eqs. (3a) and (3b). The identification results are displayed in Fig. 5 for rectangular pad, Figs. 6 and 7 for circular pad of ϕ20mm and ϕ60mm respectively. The same experiment for each type bearings is repeated three times and

Table 2 Length (L_p) and restriction constant (κ) of connecting pipes.

Recess number	1	2	3	4
L_p (m) ±5mm	2.59	2.86	3.57	2.73
κ ($10^{-11}m^3$)	1.54	1.40	1.12	1.46

shown by three types of lines in three figures. In these figures, the markers are the average of identified values. When applying load of 0 N, identified recess pressures must not be zero because have worktable weight. This identification can be verified that the recess pressures can be linear function of loads and restriction constants of connecting pipes and should be constants.

In Figs. 5 to 7, all recess pressures P_r' are not zero when $W = 0$ because recess pressure P_r' must support the worktable weight. Figures 5 and 7 for the effective areas are had larger pads, so P_r' are lower but not zero. In Fig. 6 for the smallest recess area (ϕ = 20mm), so P_r' is the largest and in Fig. 7 for the largest recess area, so P_r' is the minimum.

The pad restriction constant γ and initial film thickness $h_0 - d_0$ are determined by Eqs. (6a) and (6b) with the measurements of supply pressure P_s, flow rate Q, inlet and outlet temperatures of restrictor (T_s, T_r), and displacement average of worktable due to adding weight. Both identified values correspond to the changes of P_s (P_s = 0.5, 1, 1.5, 2MPa) as shown from Figs. 8 to 10 for three-types bearings with three times experiments which as shown by three types of lines and the markers are averages of identified values. The right column of this figure illustrates that the initial film thickness ($h_0 - d_0$) gets larger as P_s is increasing but ($h_0 - d_0$) can be kept constant when W (which changes from 0 to 2000 N) is varying as P_s (which changes from 0.5 to 2MPa) is constant. The left column illustrates that γ is kept constant when W (which changes from 0 to 2000N) or P_s (which changes from 0.5 to 2MPa) is changed.

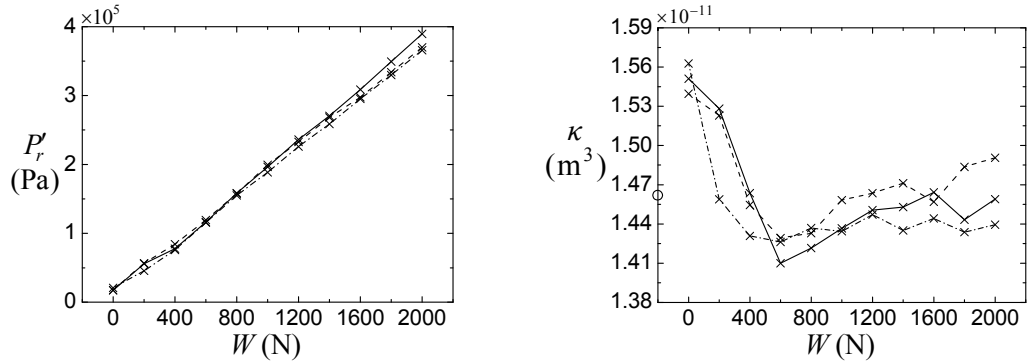
The identification Eqs. (3a), (3b), (6a) and (6b) identified the system parameters and then substituting them into rational formula can give the identified flow rates. Therefore, the differences measured exist in flow rates between the valve and identified valve due to measuring physical valve which is direct measured P_r, P_s, and Q.

For the evaluation of the identification results, a relative error ratio (rer) can be defined by

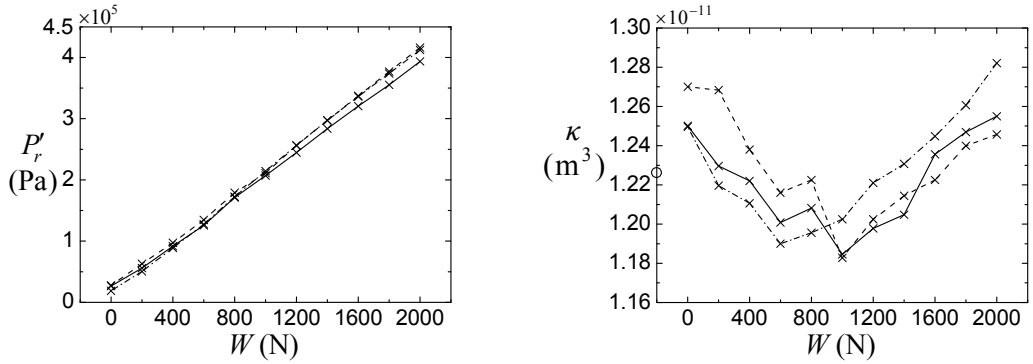
$$\text{rer} = (iv - dv) / dv \tag{12}$$

where iv and dv are denoted for identified value and designed value. The dv is determined by using Eqs. (11a) and (11b) to determined γ and using Eq. (4b) to determine initial film thickness $h_0 - d_0$ with respect to supply pressure P_s gives the results as shown in Fig. 11(a). The iv of ($h_0 - d_0$) can be determined by Eq. (6b) which using Q, d, μ and identified γ and P_r' as shown in Figs. 11(b) ~ (c). In Fig. 11, from h_1 to h_4 are measured on four locations of worktable top.

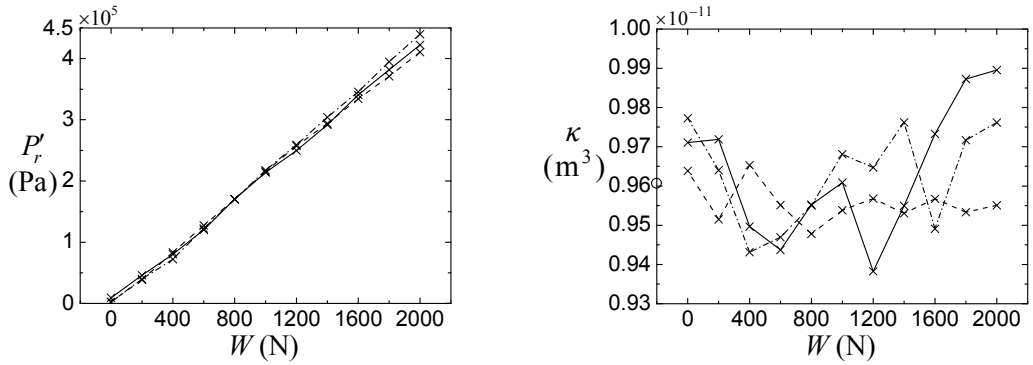
https://doi.org/10.1017/jmech.2014.91 Published online by Cambridge University Press



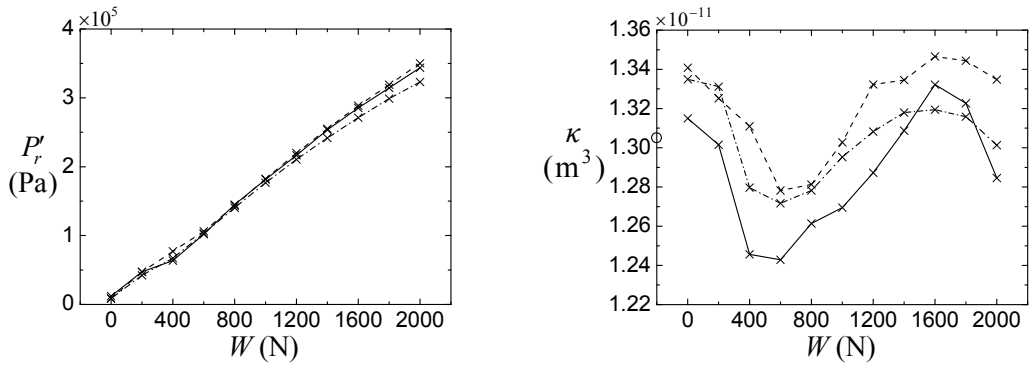
pad 1



pad 2



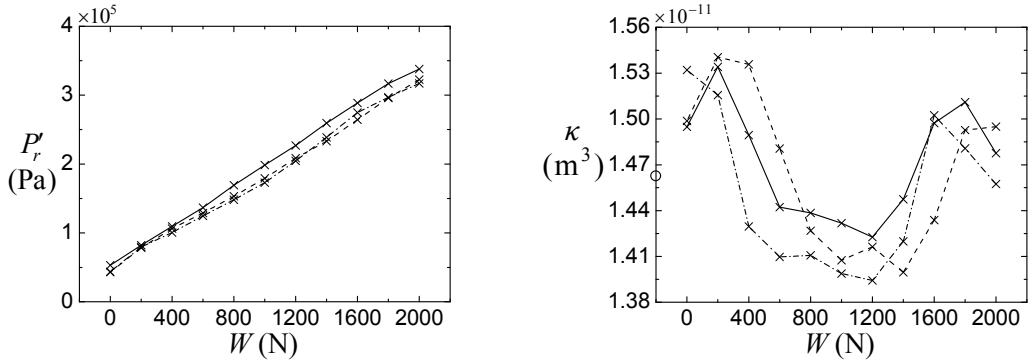
pad 3



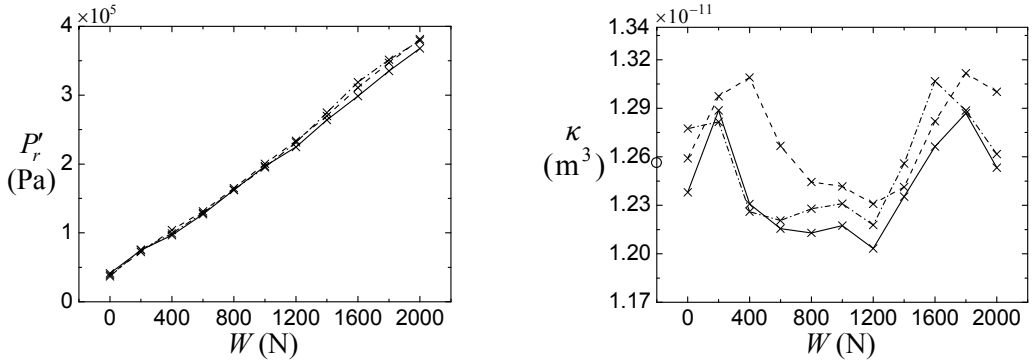
pad 4

Fig. 5 Identified results of recess pressures of pads and restriction constants of connecting pipes for rectangular pad (○ : Average of identified κ).

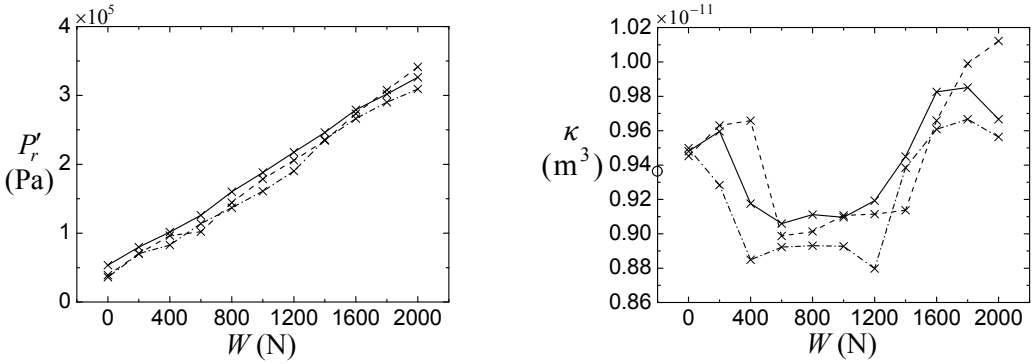
https://doi.org/10.1017/jmech.2014.91 Published online by Cambridge University Press



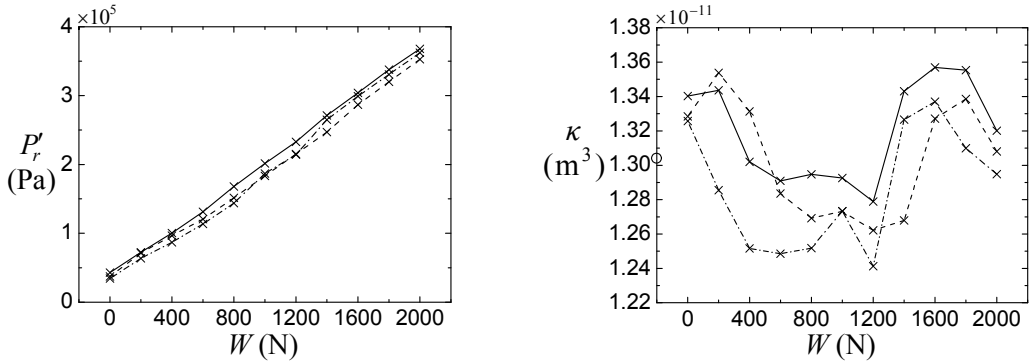
pad 1



pad 2



pad 3



pad 4

Fig. 6 Identified results of recess pressures of pads and restriction constants of connecting pipes for circular pad of ϕ20mm (○ : average of identified κ).

https://doi.org/10.1017/jmech.2014.91 Published online by Cambridge University Press

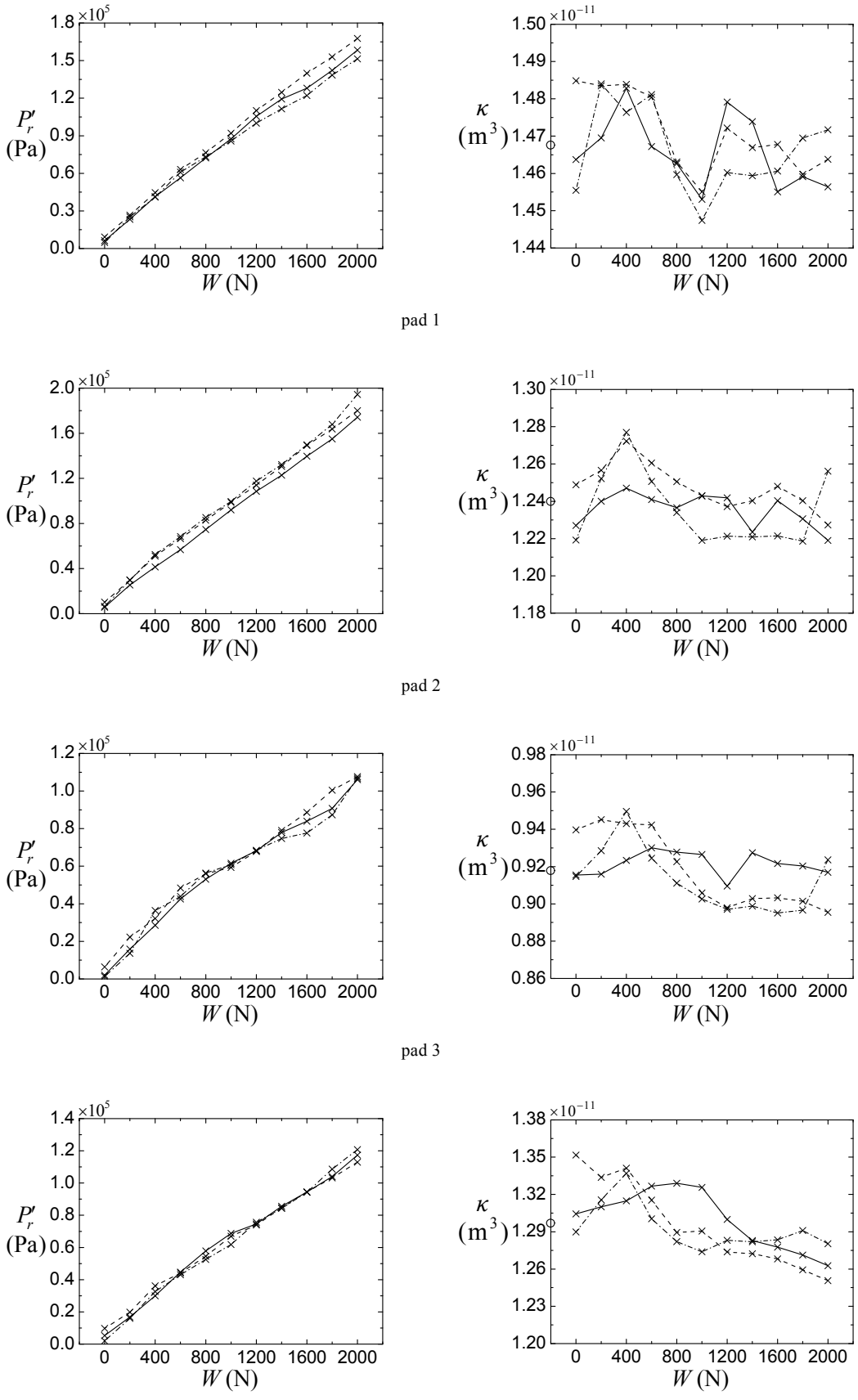
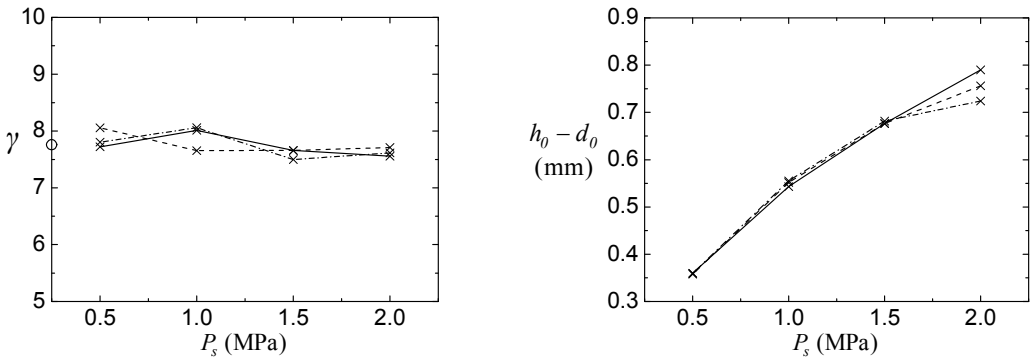
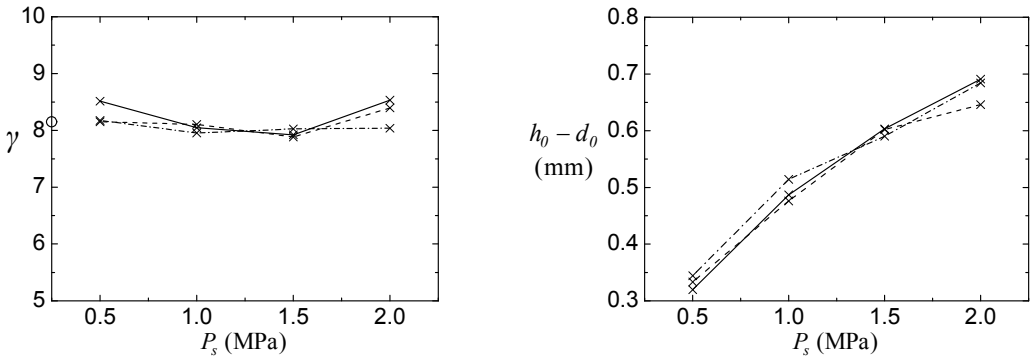


Fig. 7 Identified results of recess pressures of pads and restriction constants of connecting pipes for circular pad of ϕ60mm (○ : average of identified κ).

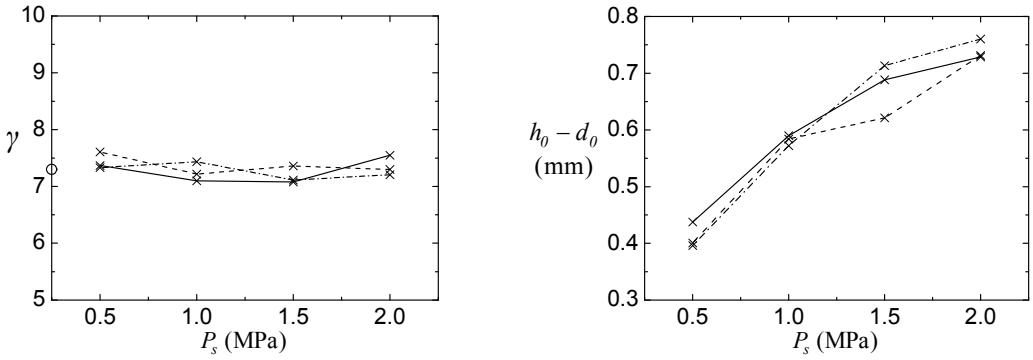
https://doi.org/10.1017/jmech.2014.91 Published online by Cambridge University Press



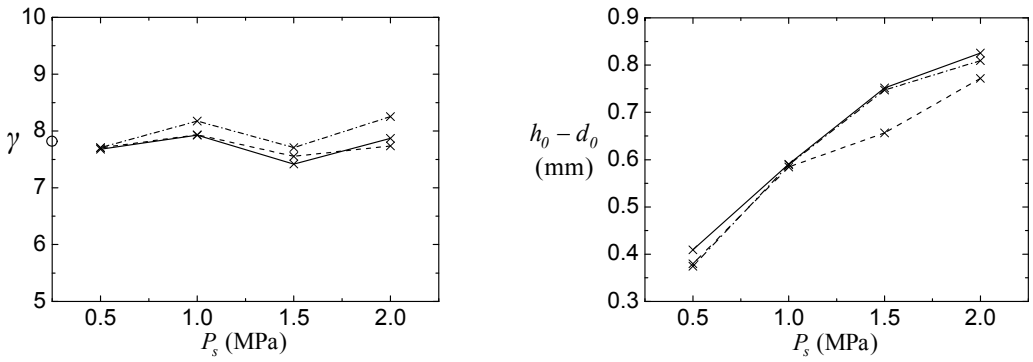
pad 1



pad 2



pad 3



pad 4

Fig. 8 Identified results of restriction constant of hydrostatic pad and initial film thickness for rectangular pad (○ : average of identified γ).

https://doi.org/10.1017/jmech.2014.91 Published online by Cambridge University Press

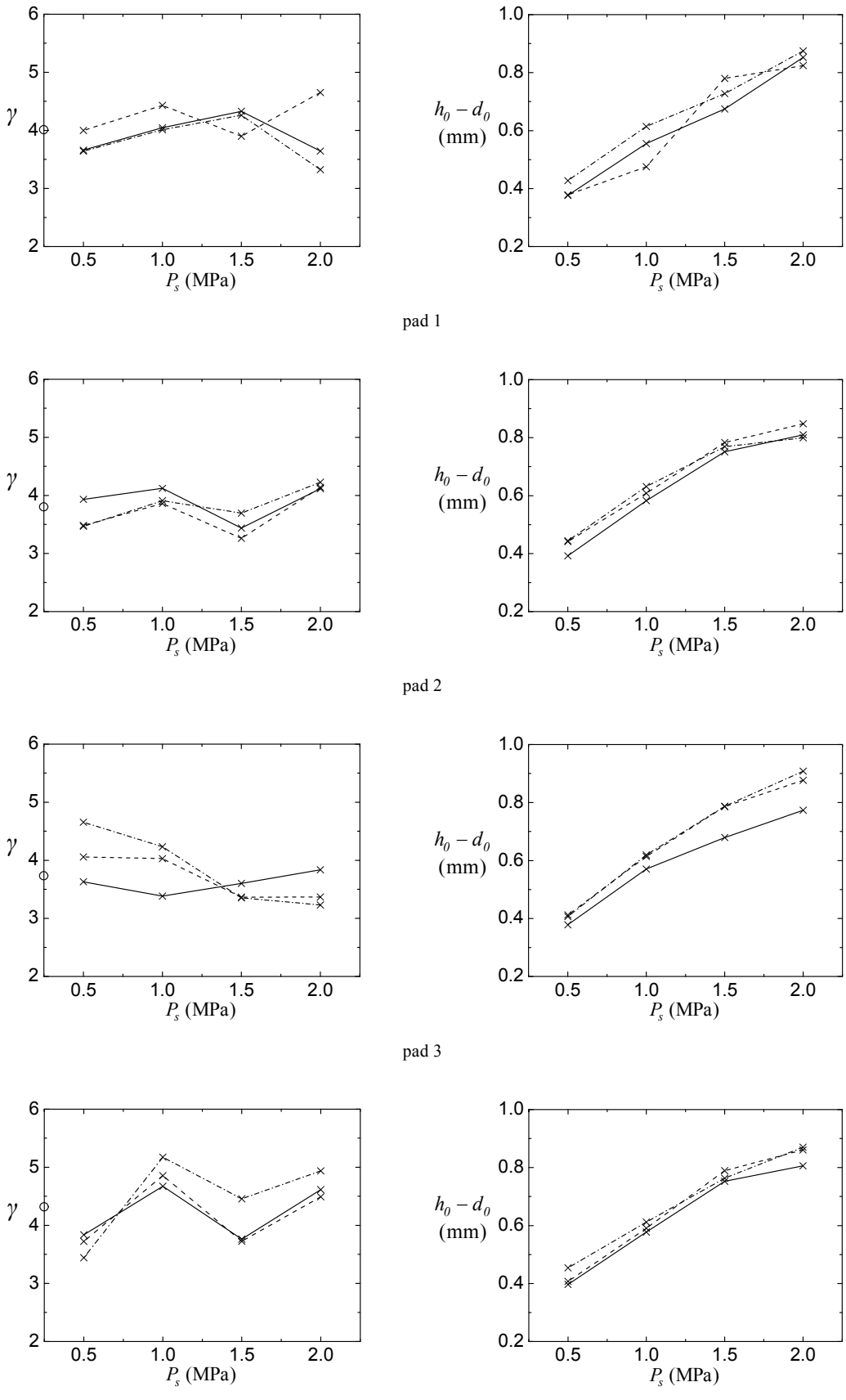
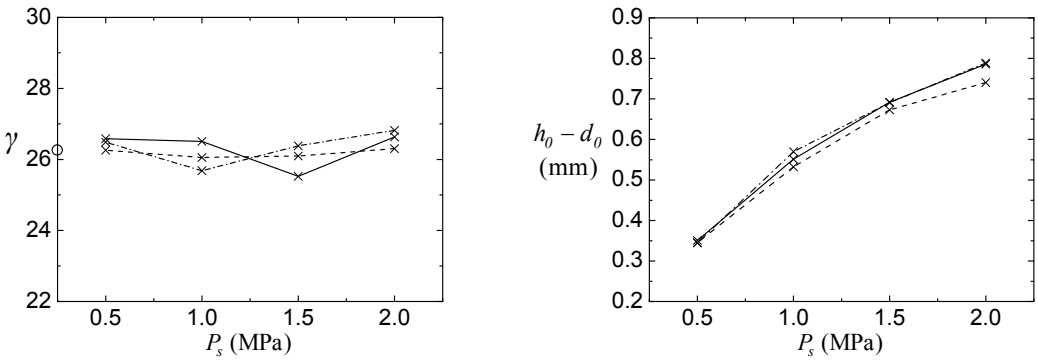
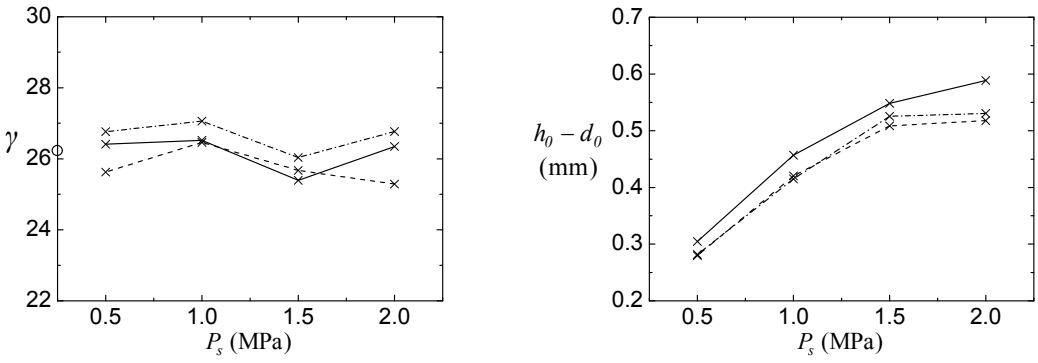


Fig. 9 Identified results of restriction constant of hydrostatic pad and initial film thickness for circular pad of ϕ20mm (○ : average of identified γ).

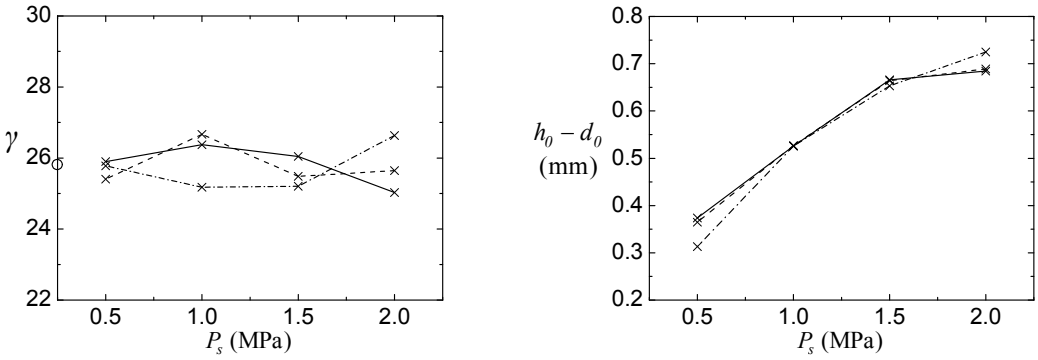
https://doi.org/10.1017/jmech.2014.91 Published online by Cambridge University Press



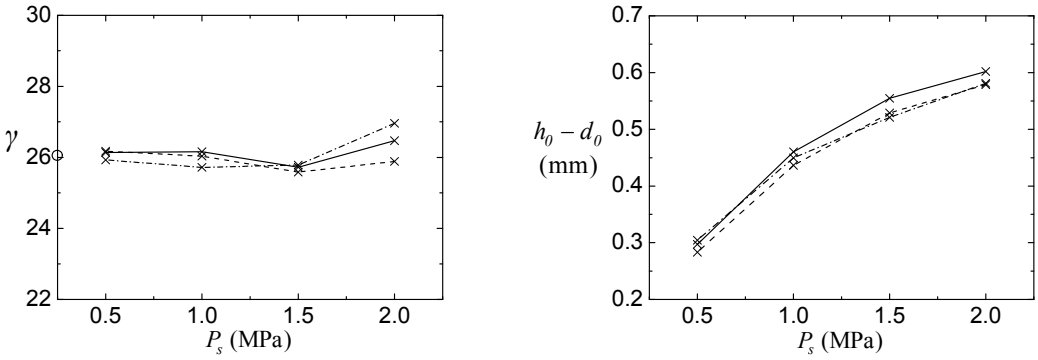
pad 1



pad 2



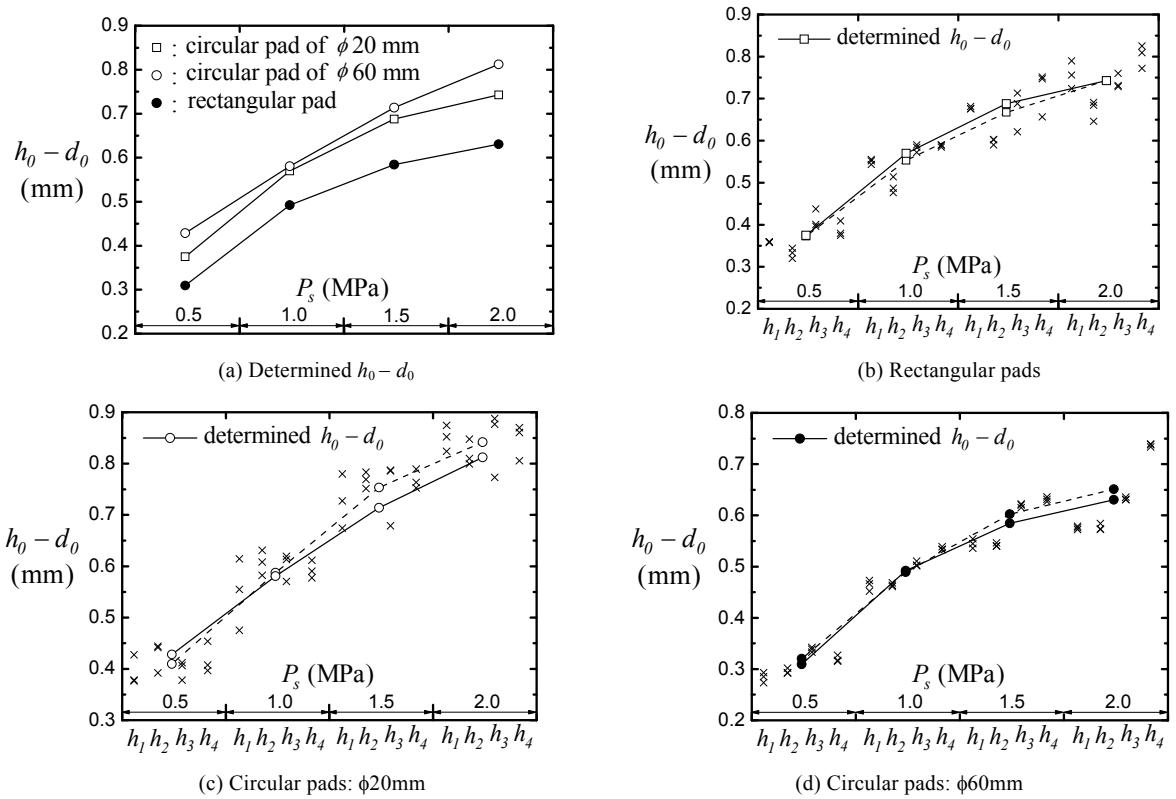
pad 3



pad 4

Fig. 10 Identified results of restriction constant of hydrostatic pad and initial film thickness for circular pad of ϕ60mm (○ : average of identified γ).

https://doi.org/10.1017/jmech.2014.91 Published online by Cambridge University Press



(a) Determined $h_0 - d_0$

(b) Rectangular pads

(c) Circular pads: ϕ20mm

(d) Circular pads: ϕ60mm

——— : Average of determinations,

– – – – : Average displacement of 11(b) ~ 11(d) comparisons determined values and identified values of $h_0 - d_0$,

× : Measurements of displacement.

Fig. 11 Identification and determination result of initial film thickness with respect to supply pressure.

Effective area of hydrostatic pad h_{eff} is defined by area providing uniform recess pressure to give equivalent load capacity of whole pad, which can be described by

$$A_{eff} = (L - \ell)(B - b) \tag{13a}$$

for rectangular pad, and

$$A_{eff} = \pi R_2^2 \left[1 - \left(\frac{R_1}{R_2}\right)\right]^2 \left(2\,\ell n \frac{R_2}{R_1}\right)^{-1} \tag{13b}$$

for circular pad. The effective areas can be determined by using Eqs. (13a) and (13b) as shown in the last row of Table 1.

For experiments in identification, the loads and the worktable weight are obtained by measuring. And recess pressure can be obtained from measuring results or identification results. Substituting both already known data into Eq. (9b) obtains effective areas A_i as shown in the left column of Fig. 12. Furthermore, substituting the identified results of effective areas, recess pressures, and total load into Eq. (10) obtains load share ratio as shown by the right column of Fig. 12.

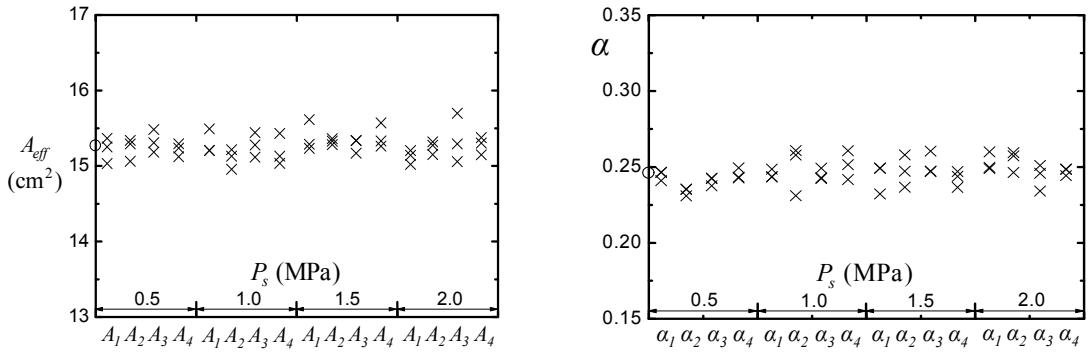
Substituting recess pressures with respect to changing W (the averages in three experiments) into Eq. (7b) gives the identified load W'. The relative error ratio of total load applied on worktable can be determined by $W' - W'/W$ which is used to evaluate the integrated error in identification results of effective areas and recess pressures.

The relative error ratios of all identified parameters including restriction constant of the connecting pipes (κ) and the restriction constant of pad (γ), initial film thickness ($h_0 - d_0$), effective areas (A_r), and loading weights (W) are determined and shown in Table 3.

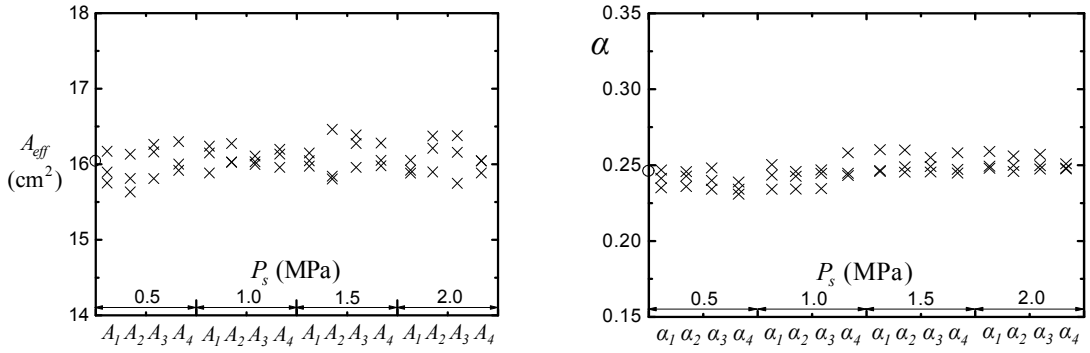
Table 3 The relative error ratio (%).

		κ	γ	$h_0 - d_0$	A_r	W
Rectangular pad	maximum	0.72	6.66	16.84	4.66	16.49
	minimum	−15.80	−11.54	−16.45	−2.29	−18.53
	mean square root	11.29	5.44	7.19	2.04	10.55
Circular pad of ϕ20mm	maximum	0.29	9.84	11.8	4.12	13.87
	minimum	−20.11	−31.44	−18.21	−2.11	12.22
	mean square root	11.55	18.6	5.73	1.95	6.83
Circular pad of ϕ60mm	maximum	3.64	1.81	25.15	3.68	20.18
	minimum	−19.64	−5.84	−17.84	−2.41	19.36
	mean square root	12.24	2.79	10.45	1.81	12.54

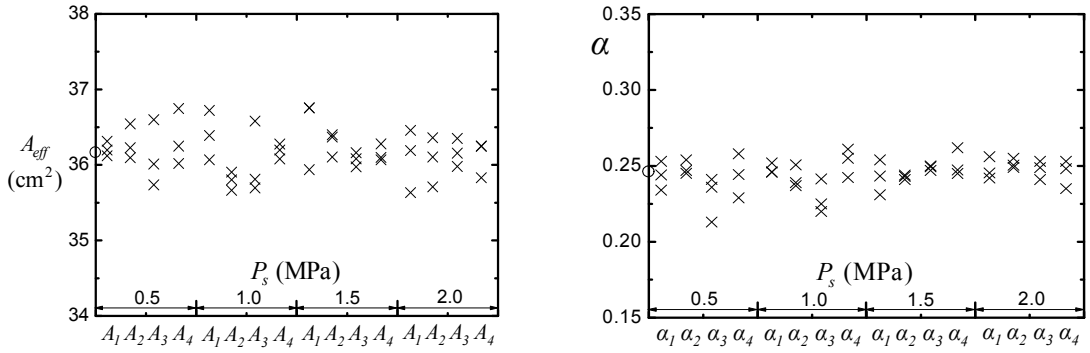
https://doi.org/10.1017/jmech.2014.91 Published online by Cambridge University Press



(a) Rectangular pad



(b) Circular pad: ϕ20mm



(c) Circular pad: ϕ60mm

Fig. 12 Effective areas and load sharing ratio (×: For three experiments, ○: Average).

5. CONCLUSIONS

This paper utilizes the method of minimizing the square error and flow theory to identify the recess pressures with respect to load increasing and restriction constant of connecting pipes. On the basis of film flow rates, dimensionless restriction parameter of the hydrostatic pads and the initial thickness of hydrostatic film can be identified to be constant and a function of the supply pressure, respectively. On the basis of load formulations, effective areas of each pad can be identified. The relative errors between identified and determined results are induced by neglecting in determination physical details, viscosity variations due to temperature change, and geometric errors caused by manufacture or design. However, the case of studies in this paper have revealed that characteristic parameters can be verified by identification results which provide the useful data to calibrate the determined values in design. The calibration results can satisfy the requirements for characteristics of hydrostatic bearings and matching-up of restrictors.

NOMENCLATURES

A_r	effective area of the r-th pad
D_p, L_p	diameter and length of connecting pipe
d	worktable displacements due to applied load
d_0	initial worktable displacement due to worktable weight
E	total error square, $E = \sum e_i^2$
e_i	error between measured and estimated flow rates
h	net film thickness
h_0	original film thickness without worktable and any load
$h_0 - d_0$	initial film thickness that it is only subjected to worktable weight without any load (mm)

https://doi.org/10.1017/jmech.2014.91 Published online by Cambridge University Press

j subscript for ordinal number of measurements
N, N' total number of measurements
n total number of pads
P_s supply pressure (Pa)
P_r, P_r' pressure at restrictor outlet and recess pressure of the r-th pad (Pa)
Q measured flow rate (cm^3/min)
Q' estimated flow rate from identification (cm^3/min)
T_r, T_r' inlet, outlet temperature (°C)
T_0 temperature at the clearance outlet (°C)
W applied load on the worktable (N)
W_0 worktable weight (N)
α_i load sharing ratio of the i-th pad
γ restriction constant of bearing pad
κ_μ restriction parameter of connecting pipe (m^5/N·s)
κ restriction constant of connecting pipe
μ absolute viscosity (N·s/m^2)

REFERENCES

1. Raimondi, A. and Boyd, J., "An Analysis of Orifice & Capillary-Compensated Hydrostatic Journal Bearings," *Journal of the American Society of Lubrication Engineering*, pp. 29–37 (1957).
2. Malanoski, S.-B. and Loeb, A.-M., "The Effect of the Method Compensation on Hydrostatic Bearing Stiffness," *Transaction of the ASME Journal of Basic Engineering*, **83**, pp. 179–187 (1961).
3. Rippel, H.-C., "Design of Hydrostatic Bearings: Part 2 — Controlling Flow with Restrictors," *Machine Design*, pp. 122–126 (1963).
4. Rippel, H.-C., "Design of Hydrostatic Bearings: Part 3 — Influence of Restrictors on Performance," *Machine Design*, pp. 132–138 (1963).
5. Kang, Y., Lee, J.-L., Huang, H.-C., Lin, C.-Y., Lee, H.-H., Peng, D.-X. and Huang, C.-C., "Design for Static Stiffness of Hydrostatic Plain Bearing: Constant Compensations," *Industrial Lubrication and Tribology*, **63**, pp. 178–191 (2011).
6. Kang, Y., Chen, C.-H., Lee, H.-H., Hung, Y.-H. and Hsiao, S.-T., "Design for Static Stiffness of Hydrostatic Plain Bearing: Single-Action Variable Compensations," *Industrial Lubrication and Tribology*, **63**, pp. 103–118 (2011).
7. Kang, Y., Lee, J.-L., Huang, H.-C., Lin, C.-Y., Lee, H.-H., Peng, D.-X. and Huang, C.-C., "Design for Static Stiffness of Hydrostatic Plain Bearing: Double-Action Spool-Type Compensations," *Industrial Lubrication and Tribology*, **66**, pp. 83–99 (2014).
8. Kang, Y., Peng, D.-X., Hung, Y.-H., Hu, S.-Y. and Lin, C.-S., "Design for Static Stiffness of Hydrostatic Bearings: Double-Action Variable Compensation of Membrane-Type Restrictors and Self Compensation," *Industrial Lubrication and Tribology*, **66**, pp. 322–334 (2014).
9. O'Donoghue, J.-P. and Rowe, W.-B., "Design of Hydrostatic Bearings Using an Operating Parameter," *Wear*, **14**, pp. 355–362 (1969).
10. Rowe, W.-B. and O'Donoghue, J.-P., "Design of Opposed-Pad Hydrostatic Bearings for Machine Tool Slideways," *Machinery and Production Engineer*, **116**, pp. 407–412 (1970).
11. Yakir, E.-M., "Regulators for Open Hydrostatic Slideways," *Machines and Tooling*, **44**, pp. 28–32 (1973).
12. Telingater, V.-S., "Hydrostatic Slideways Using Standard Bearings," *Machines and Tooling*, **43**, pp. 15–20 (1973).
13. Bushuyev, V.-V., "Angular Stiffness of Hydrostatic Slides," *Machines and Tooling*, **124**, pp. 26–29 (1973).
14. Sharma, S.-C., Jain, S.-C. and Bharuka, D.-K., "Influence of Recess Shape on the Performance of a Capillary Compensated Circular Thrust Pad Hydrostatic Bearing," *Tribology International*, **35**, pp. 347–365 (2002).
15. Kang, Y., Chou, H.-C., Wang, Y.-P., Chen, C.-H. and Weng, H.-C., "Dynamic Behaviors of a Circular Work Table Mounted on Closed Type Hydrostatic Thrust Bearing Compensated by Constant Compensations," *Journal of Mechanics*, **29**, pp. 297–308 (2013).
16. Kang, Y., Shen, P.-C., Chang, Y.-P., Lee, H.-H. and Chiang, C.-P., "Modified Predictions of Restriction Coefficient and Flow Resistance for Membrane-Tape Restrictors in Hydrostatic Bearing by Using Regression," *Tribology International*, **40**, pp. 1369–1380 (2007).
17. Kang, Y., Shen, P.-C., Chang, Y.-P. and Lee, H.-H., "Modified Determination of Fluid Resistance for Membrane-Type Restrictor," *Industrial Lubrication and Tribology*, **59**, pp. 123–131 (2007).
18. Kang, Y., Chen, C.-H., Chen, Y.-C., Chang, C. and Hsiao S.-T., "Parameter Identification for Single-Action Membrane-type Restrictors of Hydrostatic Bearings," *Industrial Lubrication and Tribology*, **64**, pp. 39–53 (2012).

(Manuscript received November 14, 2013, accepted for publication September 5, 2014.)

https://doi.org/10.1017/jmech.2014.91 Published online by Cambridge University Press